Flexible Transient Design-Oriented Model Predictive Control for Power Converters

Li, Yuan; Sahoo, Subham; Ou, Shuyu; Leng, Minrui; Vazquez, Sergio; Dragicevic, Tomislav; Blaabjerg, Frede

Published in:
I E E E Transactions on Industrial Electronics

Publication date:
2023

Document Version
Accepted author manuscript, peer reviewed version

Flexible Transient Design-Oriented Model Predictive Control for Power Converters

Yuan Li, *Student Member, IEEE,* Subham Sahoo, *Senior Member, IEEE,* Shuyu Ou, *Student Member, IEEE,* Minrui Leng, *Student Member, IEEE,* Sergio Vazquez, *Fellow, IEEE*, Tomislav Dragičević, *Senior Member, IEEE,* and Frede Blaabjerg, *Fellow, IEEE*

***Abstract*—Model predictive control (MPC) is one of the promising candidates for power converters with improved stability and faster response. Overshoot, a crucial transient precursor, is a custom design requirement based on the converters' applications having variant time-domain specifications that are subject to their safety and reliability. Apart from the generally accepted weight design process for improved settling time, when considering an MPC-controlled system, a theoretical framework to adjust the overshoot requirements has been overlooked so far. To bridge this gap, this paper proposes a new method that integrates a flexible output voltage overshoot design method into MPC-controlled dc/dc boost converters, thereby formally ensuring that the controller always complies with the time-domain specifications under dynamic disturbances. Firstly, this paper provides the MPC controller's model by deriving the optimal duty cycle value, which is then used to derive the closed-loop transfer functions. Next, the cut-off frequency is obtained based on the transfer functions. The weighting factor ratio of the MPC, which is a tunable parameter is then adjusted to ensure an adequate system's cut-off frequency. Finally, the effectiveness and ruggedness of the proposed method are validated under experimental conditions, allowing flexibility to extend its use for different power converter applications.**

***Index Terms*—Model predictive control; dynamic performance; overshoot design; cut-off frequency; weighting factors.**

I. Introduction

NOWADAYS, global ambitions of energy efficiency and carbon neutrality have put forward new design challenges in future power grids [1], [2]. In response, developments in electric vehicles (EVs), and renewable energy generation technologies have scaled up. To manage the power in such systems (EV charging stations, photovoltaic generation, etc.) more efficiently, the DC microgrid has gained a lot of academic and industrial attention [3]-[6]. A typical structure of a DC microgrid involves several dc/dc converters connected via different topologies to a DC bus, with each converter supporting different output voltage levels for various loads [6]. To ensure a stable and smooth operation of the microgrid systems, control techniques play a crucial role. Model predictive control (MPC) is one of the promising candidates to tackle the control problems of such systems, offering benefits such as improved stability, ease of implementation, explicit consideration of constraints, and other benefits [7]-[9].

Stability and dynamic performance are two vital performance indicators of power converters' operation. When looking into the stability performance, some of the typical stability issues such as instability of the system caused by the converters which act as the constant power loads have already been studied thoroughly in many previous works [10]-[12]. Considering the dynamic process, the works in [13]-[16] propose several MPC-based algorithms to improve the performance. More specifically, the authors in [13] propose a virtual power control and MPC combined algorithm to ensure an excellent dynamic response for isolated dc/dc converters. A double-loop control framework is proposed in [14] for microgrids. The inner loop with double vector MPC is utilized to track the output voltage derived from the outer loop, and this control strategy improves the control accuracy as well as the dynamic response. In [15], the solution to enhance the dynamic performance is to incorporate an additional item into the cost function. This additional item is composed of the output current, the output voltage reference as well as a weighting factor that balances the relative importance of the two items. However, a trade-off should be considered between dynamic performance and steady-state error. In [16], ANN-assisted MPC is proposed, which also selects weighting factors to enhance the dynamic response. The basic idea behind using ANN is to compare the response time with different combinations of weighting factors and then determine the optimal strategy. Although the said MPC-based control methods could enhance the dynamic performance, they cannot guarantee that the overshoot will be limited to a specific value, which affects their safety and reliability.

Dynamic overshoots exceeding the pre-specified limits may have an impact on the performance and the lifetime of equipment connected to the dc microgrids and the converters themselves [17]. Additionally, an overshoot in the output volt-

This work was partly supported by the China Scholarship Council (CSC), partly by the Baltic-Nordic Energy Research programme via Next-uGrid project, and partly by the REliable Power Electronic-Based Power System (REPEPS) project, Denmark. Minrui Leng gratefully acknowledges the financial support from the National Natural Science Foundation of China under Grant 62303334 and the Youth Fund of Sichuan Province under Grant 23NSFSC3809. Sergio Vazquez gratefully acknowledges the financial support provided by the project PID2020-115561RB-C31 funded by MCIN/AEI/10.13039/501100011033 and the project TED2021-130613B-I00 funded by MCIN/AEI/10.13039/501100011033 and by the "European Union NextGenerationEU/PRTR".

Y. Li, S. Sahoo, S. Ou and F. Blabbjerg are with the AAU Energy, Aalborg University, Aalborg, Denmark. (e-mail: yuanli, sssa, so, fbl@energy.aau.dk)

M. Leng is with the College of Electrical Engineering, Sichuan University, Chengdu, China. (e-mail: mrleng pece@163.com)

S. Vazquez is with the Laboratory of Engineering for Energy and Environmental Sustainability, Universidad de Sevilla, 41092 Sevilla, Spain (e-mail: sergi@us.es).

Tomislav Dragičević is with the Department of Electrical Engineering, Technical University of Denmark, Copenhagen, Denmark. (e-mail: tomdr@elektro.dtu.dk)

age may lead to electromagnetic interference (EMI) problems, where the high-frequency components of the overshoot within every switching period can radiate and interfere with other electronic devices and circuits, leading to malfunction and performance degradation. Furthermore, if the system is not quickly damped, stability and transient response may also degrade, resulting in oscillations that can further negatively affect the overall performance. In practical applications, the overshoot of converters is always limited within the safety specifications. For instance, the design specification of a 12 V output dc/dc boost converter limits the output overshoot below 0.6 V when the load current changes with 1.5 A under specific circuit parameters [18]. In a battery charging specification for a USB application, the maximum overshoot of the charging port is 6 V, and the maximum undershoot voltage of the same port is 4.1 V with a 5 V rated output voltage [19]. Considering an EV charging station, the output voltage overshoot should not exceed 10% of the rated output voltage in a DS/EN 61851-23 standard [20]. Additionally, the DS/EN 16603-20-20 standard specifies the allowable operational current in the electrical design and interface requirements for a power supply [21]. Moreover, the voltage deviation of pulse generators, according to ISO 7637 standard, is also illustrated with different levels from 5% - 10% based on different load conditions [22]. Therefore, when designing a system, it is necessary to consider overshoot and incorporate it into the control loop design process.

The design of an overshoot in a system can be analyzed both with the time domain and frequency domain [17]. In the time domain, a concept of state overshoot for the systems is proposed based on the overshoot definition and norm. Then, the value of the overshoot can be expressed as the absolute value of the circuit variables [17], [23]. However, this approach may not fully express the overshoot based on the sum of the absolute value of each variable due to the inherent dependency between each variable. In the frequency domain, the Bode diagram is often used to qualitatively design overshoots in dc/dc converters [24]. By deriving the cut-off frequency, the overshoot can easily be determined [18]. However, these methodologies primarily focus on PI-controlled systems, with a little discussion of extension into MPC-controlled systems. Therefore, the main objective of this paper is to achieve a specifically constrained overshoot/undershoot for the MPC-controlled system by carefully designing the parameters in the controller. Notably, the study focuses on the continuous control set (CCS)-MPC (referred to as MPC for simplicity in the text) controlled system. This algorithm is chosen for its capability to generate a fixed switching frequency, effectively mitigating issues such as high acoustic noises, operation mode uncertainty, aggressive ripples, and so on [9].

With a particular focus on flexibility induced into MPC to assist the transient design compliance, the key contributions of this paper are as follows:

1) This paper proposes a novel overshoot design method for MPC-controlled converters. The approach involves developing a small signal model to establish the relationship between the time domain specification and the system. Based on the system's cut-off frequency, the controller's parameter is determined to meet the desired overshoot specification effectively.

2) It introduces a new way for a flexible adjustment of the proposed method to satisfy the overshoot specifications. By conducting frequency domain analysis, the proposed method allows for achieving different overshoot requirements simply by modifying the ratio of weighting factors in the MPC controller. This efficient adjustment capability enables effective control of overshoot under different operating conditions.

The rest of the paper is organized as follows. Section II illustrates the basic model of the boost converter. Section III proposes the overshoot design method of the MPC-controlled system. Experiments are provided in Section IV. Section V concludes the paper and discusses several promising future directions.

II. Basic Principle of MPC controlled DC/DC Boost converter

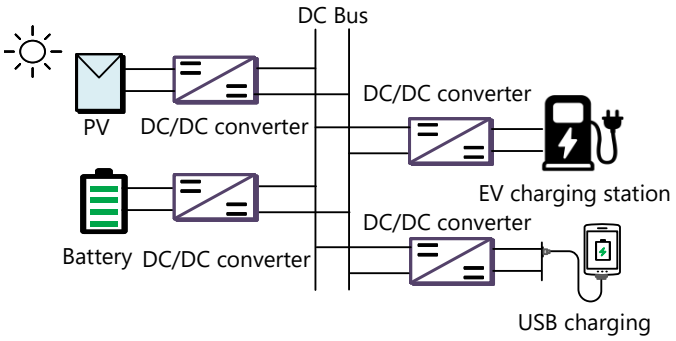

Fig. 1. A typical DC microgrid system with different types of loads and sources.

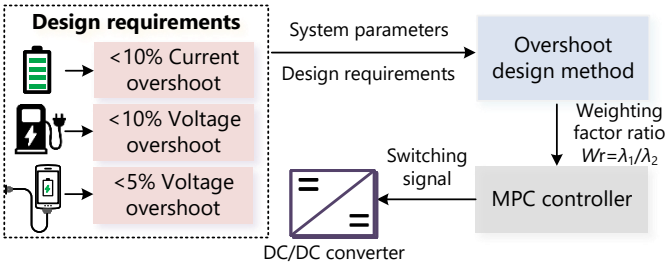

Fig. 2. Framework of the overshoot design method for MPC controlled converters.

Fig. 1 depicts a typical DC microgrid system with various types of loads. As previously mentioned, each load type has its unique overshoot requirement. Therefore, the objective is to design the MPC controller for each converter to meet their respective overshoot criteria, as illustrated in Fig. 2. The process entails the following steps: Firstly, the parameters of each system and the design requirement (overshoot/undershoot under certain current changes) are determined. Next, the design method calculates the control parameters for each MPC controller. Finally, the MPC controller generates a switching

signal to regulate the converter. In this study, the voltage level in [18] is used as a demonstration.

Fig. 3 shows a single-line diagram of the considered system, which consists of an input *LC* filter and a boost converter. The inclusion of the input *LC* filter in the system serves multiple purposes. It helps attenuate high-frequency components, thereby ensuring a cleaner and more stable input voltage to the boost converter [25]. This is especially crucial in DC microgrids where sensitive loads or other power electronics devices may be connected to the same power source. Furthermore, due to the boost converter's constant power load behavior, it is essential to avoid oscillation between the front-end system and the boost converter system. To achieve better control over the input voltage and prevent undesired interactions, an *LC* filter is equivalent to replacing the front-end converter [26]. V_g is the input voltage, V_{in} denotes the input voltage of the boost converter, i_{in} is the current across the inductor L_f and i_L is the inductor current of the boost converter, V_o represents the output voltage, i_o is the output current and R is the load. Due

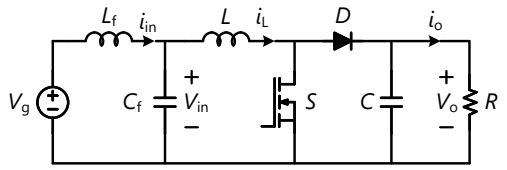

Fig. 3. DC/DC boost converter with the input LC filter.

to the following boost converter behaving as a constant power load, whose incremental impedance is negative, it tends to destabilize the system to which it is connected. That means the input port V_{in} may oscillate without any control. Therefore, the goal of the controller is to ensure stable voltages at both the input and output ports. In this paper, the difference equations are established using a single prediction horizon instead of long prediction horizons to reduce the computational burden. It should be noted that the inductor current is the control objective of the MPC-controlled boost converter to avoid non-minimum phase behavior [27],[28]. Therefore, in this paper, V_{in} and i_L are selected as the control objectives. Based on the operating principle in continuous conduction mode, the following equations can be derived:

$$\frac{di_L}{dt} = \frac{1}{L}V_{in} - \frac{1-d}{L}V_o \tag{1}$$

$$\frac{dV_{in}}{dt} = \frac{1}{C_f}i_{in}(k) - \frac{1}{C_f}i_L \tag{2}$$

where, d is the duty cycle sampled at the *kth* instant. Assuming that the sampling frequency is relatively high, the state variables can be transformed into a discrete-time equation with the classical forward Euler approximation method. The difference equations containing two objectives (inductor current i_L and input port voltage V_{in}) are provided as:

$$i_L(k+1) = i_L(k) + \frac{V_{in}(k) - V_o(k)}{L}T_s + \frac{dV_o(k)}{L}T_s \tag{3}$$

TABLE I
OPEN LOOP TRANSFER FUNCTIONS OF THE BOOST CONVERTER.

Open loop transfer functions	Values
Input current-to-inductor current G_{ii}	$\frac{1}{L_fC_fs^2+1}$
Input voltage-to-output voltage G_{vg}	$\frac{R(1-D)}{Ls(CRs+1)+R(1-D)}$
Duty ratio-to-output voltage G_{vd}	$\frac{RV_o(1-D)-\frac{V_o}{1-D}Ls}{Ls(CRs+1)+R(1-D)}$
Input voltage-to-inductor current G_{ig}	$\frac{CRs+1}{Ls(CRs+1)+R(1-D^2)}$
Duty ratio-to-inductor current G_{id}	$\frac{V_o(CRs+2)}{Ls(CRs+1)+R(1-D^2)}$

$$\begin{aligned} V_{in}(k+1) =& V_{in}(k) + \frac{i_{in}(k) - i_L(k)}{C_f}T_s \\ & - \frac{V_{in}(k) - V_o(k) - dV_o(k)}{LC_f}T_s \end{aligned} \tag{4}$$

where, T_s denotes the switching cycle. The cost function can be derived as:

$$J = \lambda_1(i_L(k+1) - i_L^*)^2 + \lambda_2(V_{in}(k+1) - V_{in}^*)^2 \tag{5}$$

where, λ_1 and λ_2 are the weighting factors, i_L^* denotes the inductor current reference and V_{in}^* represents the reference of the input voltage of the boost converter. In order to minimize the cost function, the derivative of the cost function to the duty cycle should satisfy:

$$\frac{\partial J}{\partial d} = 0 \tag{6}$$

In this case, the optimal duty cycle value can be obtained according to the chain rule:

$$\begin{aligned} d =& \frac{(V_{in}(k) + \frac{i_{in}(k) - i_L(k) - \frac{V_{in}(k) - V_o(k)}{L}T_s}{C_f}T_s - V_{in}^*)}{(\frac{\lambda_1}{\lambda_2} + \frac{T_s^2}{C_f^2})\frac{V_o(k)}{LC}} \\ & - \frac{\frac{\lambda_1}{\lambda_2}(i_L(k) + \frac{V_{in}(k) - V_o(k)}{L}T_s - i_L^*)}{(\frac{\lambda_1}{\lambda_2} + \frac{T_s^2}{C_f^2})\frac{V_o(k)}{L}T_s} \end{aligned} \tag{7}$$

This optimal value of the duty cycle is modulated to generate a switching signal for the boost converter. To clarify whether the cost function J equals its minimum value when adopting the optimal variable d, the second derivative is utilized as follows:

$$\frac{\partial^2 J}{\partial d^2} = 2\lambda_1\frac{V_o^2(k)T_s^2}{L^2} + 2\lambda_2\frac{V_o^2(k)}{L^2C^2}T_s^2 > 0 \tag{8}$$

The control variable d is in the specified range (0, 1). Referring to equation (8), it is evident that the second-order derivative of the cost function to d is positive. Consequently, the cost function attains its minimum value by adopting the derived optimal value for d. By interconnecting the control loop and power stage loop using (7), the theoretical basis for the modeling process can be established in the subsequent step.

TABLE II
SYSTEM PARAMETERS OF THE DC/DC BOOST CONVERTER.

Parameters	Symbols	Values
Input voltage	V_g	10 V
Output voltage	V_o	12 V
LC Inductance	L_f	0.8 mH
LC Capacitor	C_f	15 μF
Inductance	L	1.5 mH
Capacitor	C	2000 μF
Switching cycle	T_s	100 μs
Output current	i_o	0.5A-2A
Output voltage reference	V_o^*	12 V
Inductor current reference	i_L^*	$V_o^* i_o(k)/V_g$
Input voltage reference	V_{in}^*	10 V

III. OVERSHOOT DESIGN OF THE MPC CONTROLLED CONVERTER

A. Modeling of the MPC Controlled Converter

To ensure a safe operation of a system, it is important to carefully consider the overshoot of the output voltage when the load changes. Overshoot can be predicted using the crossover frequency of the closed-loop system, which can reveal the system's adaptive ability during the dynamic process. In this study, the cut-off frequency is employed as an alternative to the crossover frequency. This choice is made because the cut-off frequency f_c signifies that the loop gain is below the unit value, thereby indicating an inadequate attenuation of disturbances [29]. Additionally, the cut-off frequency provides information about the system's bandwidth, thereby aiding in subsequent design considerations [30].

Its relationship can be presented as [18]:

$$\Delta V_o = \frac{\Delta I_o}{2\pi f_c C} \tag{9}$$

where, ΔV_o is the output voltage overshoot, ΔI_o denotes the output current variation and f_c is the cut-off frequency. Although predicting the overshoot can be complicated by the nonlinear behavior of the MPC-based systems, it provides a clear expression for the optimal duty cycle value based on the sampled value and system parameters in (7). By introducing a small perturbation and neglecting higher-order perturbations, a small-signal equation can be obtained to analyze the system's response to changes in the load. This can help to predict and manage the overshoot in a more efficient and reliable manner.

By introducing the small-signal perturbation, (7) can be re-written as:

$$\begin{aligned} D+\hat{d} = & \\ & \frac{(V_{in}+\hat{v}_{in}+\dfrac{I_{in}+\hat{i}_{in}-I_L-\hat{i}_L-\dfrac{V_{in}+\hat{v}_{in}-V_o-\hat{v}_o}{L}T_s}{C_f}T_s)}{(\dfrac{\lambda_1}{\lambda_2}+\dfrac{T_s^2}{C_f^2})\dfrac{V_o+\hat{v}_o}{LC}} \\ & -\frac{\dfrac{\lambda_1}{\lambda_2}(I_L+\hat{i}_L+\dfrac{V_{in}+\hat{v}_{in}-V_o-\hat{v}_o}{L}T_s-I_L^*-\hat{i}_L^*)}{(\dfrac{\lambda_1}{\lambda_2}+\dfrac{T_s^2}{C_f^2})\dfrac{V_o+\hat{v}_o}{L}T_s} \\ & -\frac{V_{in}^*+\hat{v}_{in}^*}{(\dfrac{\lambda_1}{\lambda_2}+\dfrac{T_s^2}{C_f^2})\dfrac{V_o+\hat{v}_o}{LC}} \end{aligned} \tag{10}$$

Based on (10) and replacing the $\hat{i}_L^*$ with the expression of $\hat{v}_o^*$, neglecting high-order perturbations, the following equation can be obtained:

$$\begin{aligned} \hat{d} = & F_m(F_g\hat{v}_{in}+F_i\hat{i}_{in}+F_L\hat{i}_L+(F_v+F_o)\hat{v}_o \\ & +F_{inref}\hat{v}_{in}^*+F_{vref}\hat{v}_o^*) \end{aligned} \tag{11}$$

where, $F_m = 1$, $F_i = kT_s^2/C_f^2$,
$F_g = k(1-1/(LC_f)T_s^2)T_s/C_f - \lambda_1 T_s/(\lambda_2 L)$,
$F_L = -kT_s^2/C_f^2 - \lambda_1/\lambda_2$,
$F_v = k(1-D)T_s^3/(LC_f^2) + \lambda_1 T_s/(\lambda_2 L)$,
$F_o = kv_o^*/V_{in}R$, $F_{vref} = k\lambda_1/\lambda_2$,
$F_{inref} = kT_s/(C_f V_o V_{in} R)$,
$k = 1/(V_o(k)\frac{T_s}{L}(\lambda_1/\lambda_2 + T_s^2 C_f^2))$.

We define that G_{ii} represents the input current-to-inductor current transfer function, G_{vg} denotes the input voltage-to-output voltage transfer function, G_{vd} is the duty ratio-to-output voltage transfer function, G_{ig} stands for the input voltage-to-inductor current transfer function, and the duty ratio-to-inductor current transfer function is represented as G_{id}. The expressions of these open loop transfer functions are provided in Table I. Using (11), the model of the MPC-controlled boost converter is shown in Fig. 4.

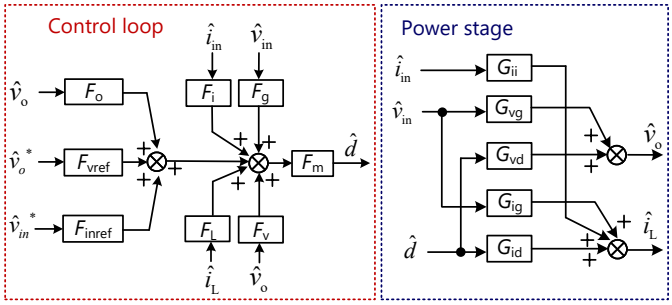

(a) (b)

Fig. 4. Small signal diagram of the MPC controlled boost converter. (a) Control loop small signal diagram. (b) Power stage small signal diagram.

Typically, the cut-off frequency is obtained from the closed-loop transfer function. Therefore, it needs to derive the transfer

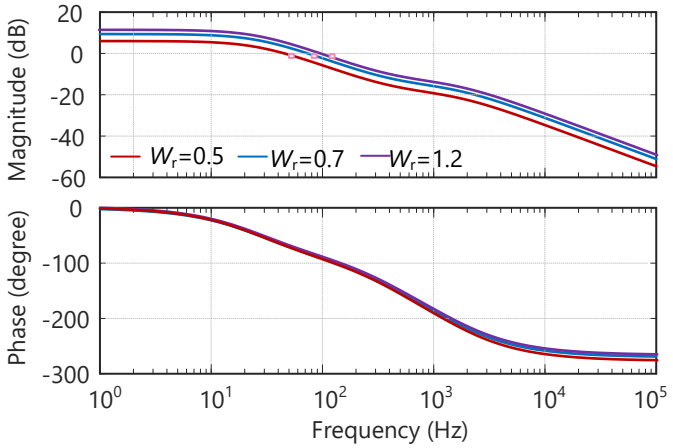

Fig. 5. Bode plots of the output voltage reference to output voltage transfer function G_{vr} with different weighting factor ratios – an increase in the weighting factor ratio results in a higher cut-off frequency.

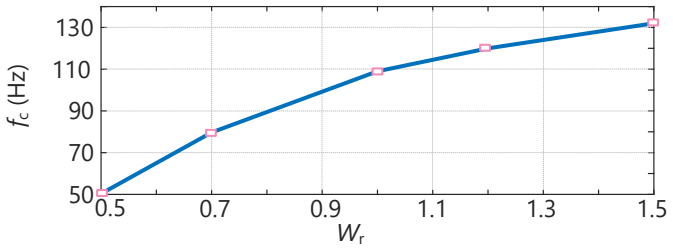

Fig. 6. The cut-off frequencies with different weighting factor ratios.

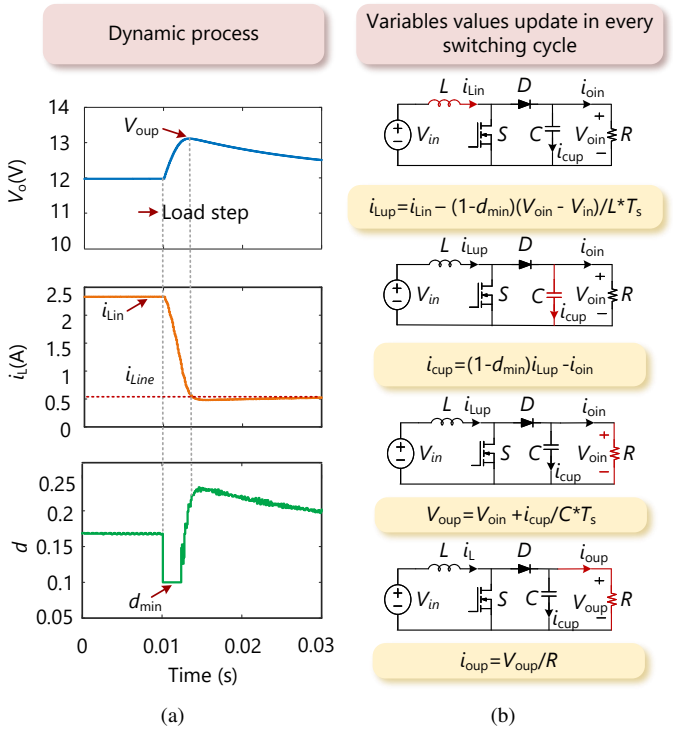

(a) (b)

Fig. 7. Calculation of the minimum output voltage overshoot. (a) Dynamic response process. (b) Variables value updating process.

function of the output voltage reference to the output voltage, as it forms a part of the control loop, as shown in Fig. 4. Setting the input perturbation $\hat{v}_{in}$, $\hat{i}_{in}$ and $\hat{v}_{in}^{*}$ to zero, the closed-loop output voltage reference $\hat{v}_o^{*}$ to output voltage $\hat{v}_o$ transfer function G_{vr} can be obtained as:

$$G_{vr} = F_m \frac{G_{vd}F_{vref}}{1-(F_v+F_o)G_{vd}-F_L G_{id}} \tag{12}$$

Based on (12), selecting the weighting as λ_1=0.5, λ_2=1, the cut-off frequency f_c can be obtained using:

$$20\log_{10} G_{vrloop}(s=f_c) = -3\text{dB} \tag{13}$$

Here, G_{vrloop} denotes the control loop of the G_{vr}. However, in practical and industrial environments, the cut-off frequency will vary with different system parameters, especially the inductance, and capacitor. In this study, to simplify the control and analysis, a fixed inductor value and a fixed capacitor value are considered, which are listed in Table II. It is also worth noting that the load resistance can also have an impact on the cut-off frequency. Typically, during the design phase, the rated load is used as a basis for this parameter, which can be obtained from specifications or through measurements [31], [32]. Furthermore, the maximum overshoot limitation is set as 1.5 V. Based on this assumption, it can be calculated that $f_c \approx 50$ Hz. Therefore, to ensure that the system meets the design specification, which stipulates that the voltage overshoot should be below 1.5 V when the load current changes by 1.5 A, it needs to determine the minimum cut-off frequency f_{cm}.

To reach the design compliance, the minimum cut-off frequency can be calculated as follows:

$$f_{cm} = \frac{1.5}{2\pi \times 1.5 \times 2000 \times 10^{-6}} \approx 80 \text{ Hz} \tag{14}$$

It can be observed that the required minimum cut-off frequency f_{cm} is higher than the calculated value of f_c. This means that the system as currently designed will not meet the overshoot design requirement, which will exceed the maximum allowable voltage overshoot. Therefore, the system needs to adjust its parameters to increase the cut-off frequency.

B. Design of the cut-off frequency

In practical applications, some parameters of a system may be fixed and can be difficult to modify. However, adjusting the parameters in the control loop is possible, which can have a significant impact on the system's behavior. In (12), it can be seen that the transfer function G_{vr} can be modified by adjusting the weighting factors. Since the cost function only involves two weighting factors, the ratio of these factors can be employed to alter λ_1. By setting λ_2 to unity and varying λ_1, the weighting factor ratio $W_r = \lambda_1/\lambda_2$ can be modified. Fig. 5 and Fig. 6 demonstrate the relationship between the weighting factor ratio and cut-off frequency, indicating that an increase in the weighting factor ratio results in a higher cut-off frequency.

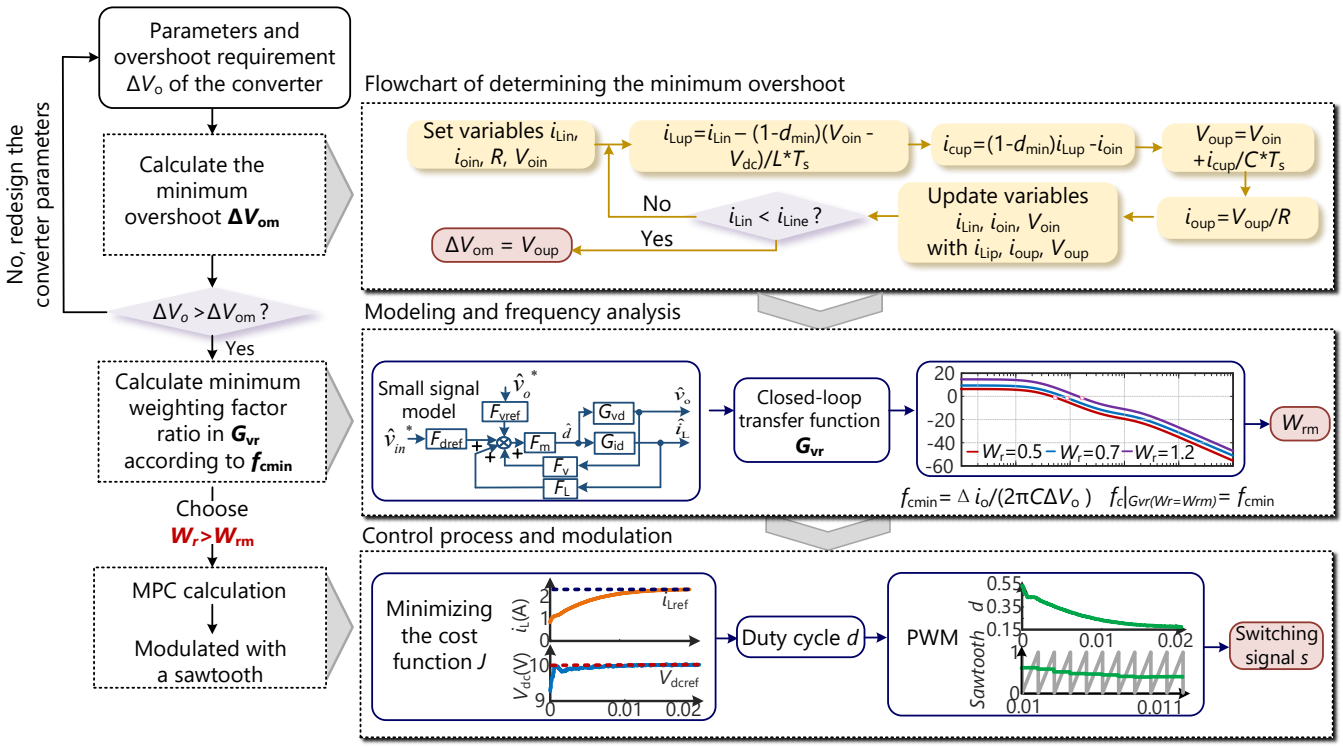

Fig. 8. Flowchart of the overshoot design process of the dc/dc boost converter.

Hence, a minimum weighting factor ratio W_{rm} can be determined as:

$$20\log_{10} G_{vrloop}(s = f_{cm}, \frac{\lambda_1}{\lambda_2} = W_{rm}) = \text{-3 dB} \qquad (15)$$

The derived value of W_{rm} is approximately 0.7, implying that if the weighting factor ratio exceeds 0.7, the cut-off frequency f_c will exceed 80 Hz. Reflecting on the time domain, it means that the output voltage overshoot resulting from load changes of 1.5 A can be effectively limited to under 1.5 V.

Although increasing the weighting factor ratio can result in a higher cut-off frequency, there exist limitations to the control system's ability to reduce the overshoot even further. This is primarily due to the fact that the duty cycle of the system is always constrained within a certain range, such as the interval $d \in [0.1, 0.9]$ in this study. Consequently, the minimum achievable overshoot can be determined by analyzing the dynamic process of the system.

The system's performance during load changes is shown in Fig. 7. It can be observed that the overshoot reaches its peak value when the inductor current i_L arrives at its new steady-state value. The dynamic process can be described as follows: at the instant when the load changes, the output current changes, which is defined as i_{oin}. Next, the inductor current decreases with the limited minimum duty cycle of 0.1 in one switching cycle, and this is defined as i_{Lup}. Then, the capacitor current i_{cup} decreases, and the overshoot of the output voltage within one switching cycle can be derived based on capacitor current i_{cup}. Finally, the output voltage becomes the updated output voltage v_{oup} and the output current is updated as i_{oup}. The above iterations are repeated until the inductor i_L current reaches its new equilibrium value i_{Line}. The iteration process and related equations are expressed with a flowchart, as shown in Fig. 8. In the studied system, the minimum overshoot can be calculated as 0.9 V.

Based on this, the overall design process is complete, as shown in Fig. 8. Firstly, the parameters and overshoot design specification ΔV_o are received. The next step is to obtain the minimum ΔV_{om} based on the minimum overshoot calculation process in Fig. 7. If ΔV_o is smaller than ΔV_{om}, the system needs to re-design the parameters. If ΔV_o is larger than ΔV_{om}, then the closed-loop transfer function is derived, and the minimum weighing factor ratio W_{rm} can be obtained. Finally, the weighting factor ratio W_r is selected to be larger than W_{rm} and updated in the MPC controller. In summary from Fig.8, the proposed method initiates by establishing a clear relationship between the parameters of the MPC controller and the system's output overshoot. This approach offers effective and flexible design capabilities for the overshoot structurally, allowing the system to achieve specific target values. Furthermore, owing to the absence of supplementary constraints and conditions during the design process, this method exhibits versatility and applicability across diverse systems.

C. Validation of the Proposed Overshoot Design Method

To support the above-mentioned analysis, Fig. 9 shows the simulations utilizing the parameters in Table II with different weighting factor ratios. As observed in the figure, when adopting a weighting factor ratio of $W_r = 0.6$, the overshoot of the output voltage is 1.7 V. Based on the analysis of the relationship between cut-off frequency and weighting factors ratio in Fig. 6, the overshoot should be $\Delta V_o = 1.5/(2\pi * 70 * 2000 * 10^{-6}) = 1.7$ V. As seen in the figure, when adopting a weighting factor ratio of $W_r = 0.7$, the overshoot of the output voltage is 1.6 V. Based on the analysis of the relationship between cut-off frequency and

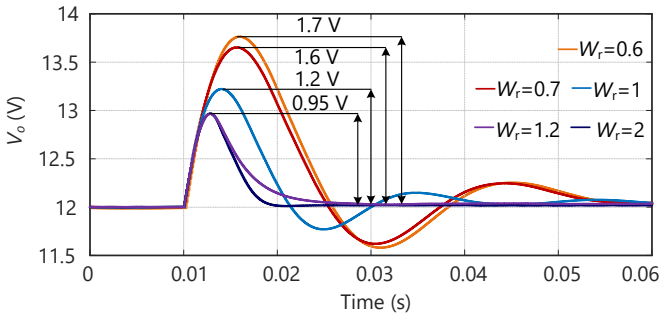

Fig. 9. Output voltage using different weighting factors ratio W_r during dynamic process with the parameters in Table II.

weighting factors ratio in Fig. 6, the overshoot should be $\Delta V_o = 1.5/(2\pi{*}80{*}2000{*}10^{-6}) = 1.5$ V. When adopting the weighting factor ratio of $W_r = 1$, the overshoot of the output voltage is 1.1 V. From the bode plot analysis, the overshoot should be $\Delta V_o = 1.5/(2\pi * 110 * 2000 * 10^{-6}) = 1.2$ V. Next, when adopting the weighting factor ratio of $W_r = 1.2$, the overshoot is 0.95 V. From the bode plots analysis, the overshoot should be $\Delta V_o = 1.5/(2\pi * 120 * 2000 * 10^{-6}) = 1$ V. Finally, due to the limitations of the adjusting ability, when adopting the weighting factor ratio of $W_r = 2$, the output overshoot equals to that when adopting $W_r = 1.2$.

From the simulation results in Fig. 9, it can be concluded that the proposed method can be utilized to design the output voltage overshoot. Adjusting the weighting factor ratio can modify the system's behavior to meet specific design requirements. Additionally, it is essential to consider the control system's adjusting ability limitations and the dynamic process characteristics.

IV. Experimental Results

To validate the analysis, a dc/dc boost converter system has been built in the lab. The DC source used in the experiment is a Delta Elektronika SM 600-10 DC power supply. The MPC algorithm is implemented using the dSPACE DS1202 board. Additionally, a PWM Generation is used to generate a 10 kHz sawtooth for generating the desired PWM. The experimental prototype consists of an LC filter followed by the boost converter, as shown in Fig. 10. Table II provides the system's parameters and the control parameters used in the experiments.

A. Case Study 1: Input voltage stability validation with MPC algorithm

A comparative evaluation was conducted to demonstrate the necessity of controlling the input port voltage V_{in} in the system. In the first test, the MPC algorithm only controlled the inductor current of the LC filter connected boost converter. As predicted, the converter which behaves as a CPL, led to oscillations in the system, as shown in Fig. 11(a).

In the second test, the MPC algorithm was used, which also controls the input voltage. As a result, the input voltage was stabilized, as shown in Fig. 11(b). These results clearly demonstrate that controlling both the input voltage and the inductor current is essential for achieving a stable performance in the studied system.

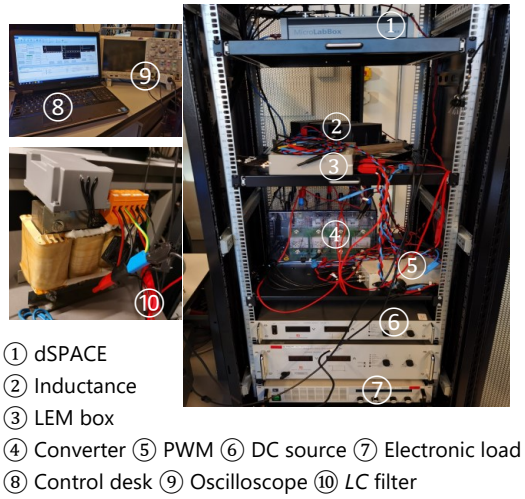

Fig. 10. Experimental setup for DC/DC converter.

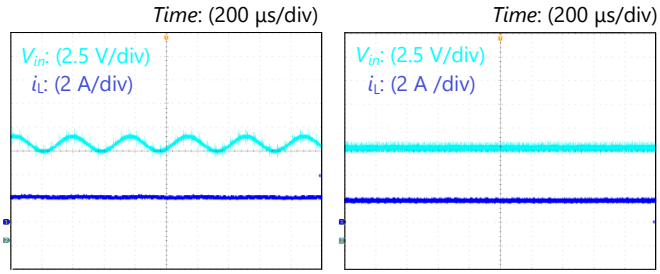

(a) (b)

Fig. 11. Input voltage V_{in} and inductor current i_L of the boost converter.(a) Without controlling the input voltage. (b) With controlling the input voltage.

B. Case Study 2: Output voltage overshoot with different weighting factor ratios

This case study validates the proposed method when the load changes using different weighting factor ratios. As discussed in Section III, when the weighting factor ratio W_r is larger than 0.7, the overshoot can be limited to 1.5 V.

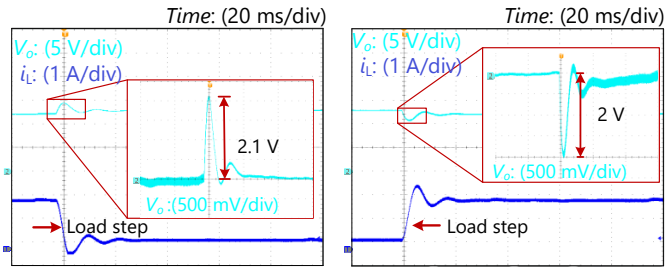

(a) (b)

Fig. 12. Output voltage overshoot and undershoot ΔV_o and the inductor current i_L of the boost converter with open loop. (a) Overshoot of the output voltage when the load current steps down to 0.5 A. (b) Undershoot of the output voltage when the load current steps up to 2 A .

Firstly, the open loop dynamic process is presented in Fig. 12. As seen, the overshoot and the undershoot during the load step are approximately 2.1 V and 2 V respectively.

Fig. 13 shows the waveforms of the system with a weighting factor ratio $W_r = 0.6$. Compared with the open loop, the overshoot is reduced to 1.7 V. Fig. 14 provides the waveforms

of the condition that $W_r = 0.7$, where the output overshoot equals 1.6 V approximately. From the analysis and simulation results in Section III, the overshoot derived is 1.6 V in this case. Fig. 15 provides the waveforms of the condition that $W_r = 0.8$, where the output overshoot equals to 1.5 V approximately. And the result is approximately corresponding to the analysis in Section III. To obtain a smaller overshoot, W_r is further increased in Fig. 16 which equals 1. As seen, the overshoot is decreased to 1.2 V. Finally, when W_r is increased significantly to 2 in Fig. 17, the overshoot is decreased to 1 V. Because of the duty cycle limitation, the overshoot cannot be further decreased.

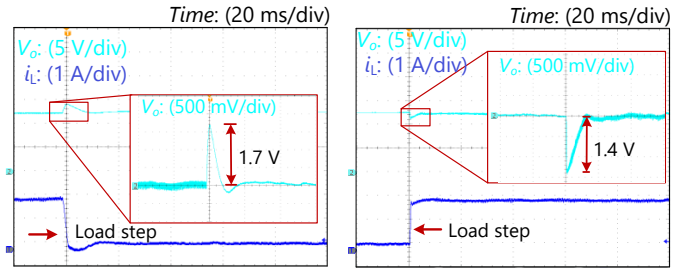

(a) (b)

Fig. 13. Output voltage overshoot and undershoot ΔV_o and the inductor current i_L of the boost converter with $W_r = 0.6$. (a) Overshoot of the output voltage when the load current steps down to 0.5 A. (b) Undershoot of the output voltage when the load current steps up to 2 A.

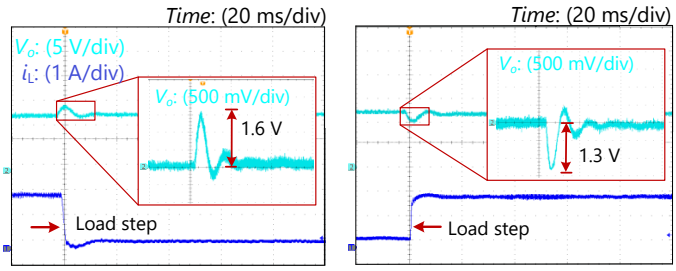

(a) (b)

Fig. 14. Output voltage overshoot and undershoot ΔV_o and the inductor current i_L of the boost converter with $W_r = 0.7$. (a) Overshoot of the output voltage when the load current steps down to 0.5 A. (b) Undershoot of the output voltage when the load current steps up to 2 A.

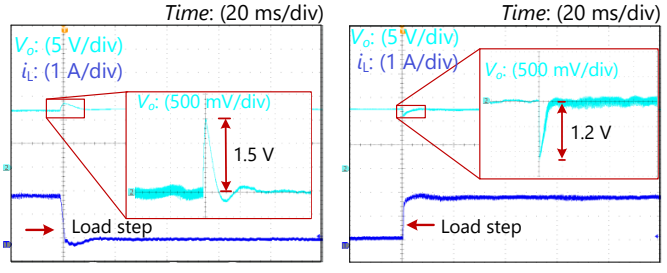

(a) (b)

Fig. 15. Output voltage overshoot and undershoot ΔV_o and the inductor current i_L of the boost converter with $W_r = 0.8$. (a) Overshoot of the output voltage when the load current steps down to 0.5 A. (b) Undershoot of the output voltage when the load current steps up to 2 A.

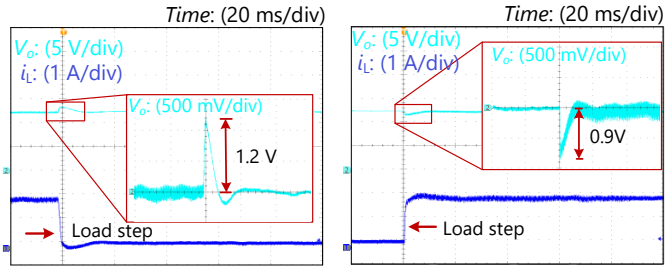

(a) (b)

Fig. 16. Output voltage overshoot and undershoot ΔV_o and the inductor current i_L of the boost converter with $W_r = 1$. (a) Overshoot of the output voltage when the load current steps down to 0.5 A. (b) Undershoot of the output voltage when the load current steps up to 2 A.

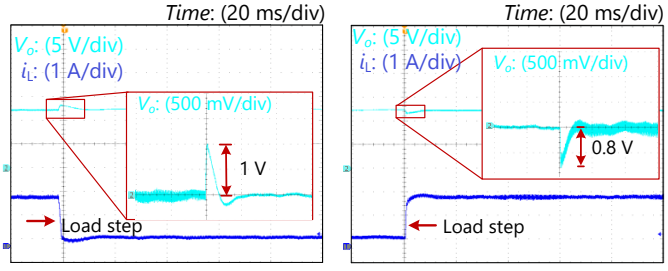

(a) (b)

Fig. 17. Output voltage overshoot and undershoot ΔV_o and the inductor current i_L of the boost converter with $W_r = 2$. (a) Overshoot of the output voltage when the load current steps down to 0.5 A. (b) Undershoot of the output voltage when the load current steps up to 2 A.

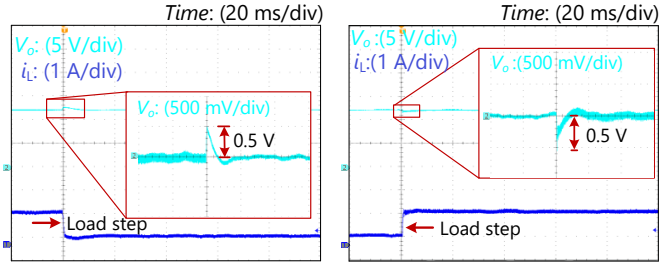

(a) (b)

Fig. 18. Output voltage overshoot and undershoot ΔV_o and the inductor current i_L of the boost converter with $W_r = 2$. (a) Overshoot of the output voltage when the load current steps down to 0.6 A. (b) Undershoot of the output voltage when the load current steps up to 1.5 A.

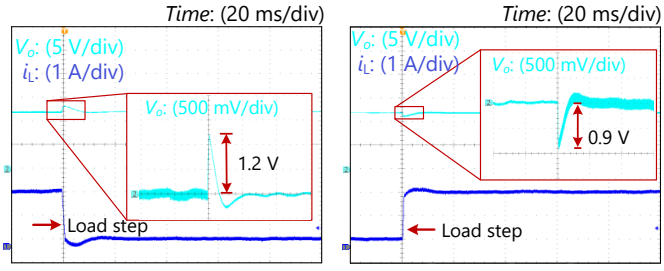

(a) (b)

Fig. 19. Output voltage overshoot and undershoot ΔV_o and the inductor current i_L of the boost converter with $W_r = 2$ and the input voltage V_{in} = 9 V. (a) Overshoot of the output voltage when the load current steps down. (b) Undershoot of the output voltage when the load current steps up.

C. Case Study 3: Output voltage overshoot (undershoot) with different load changes and input voltages

In real applications, the input voltage and load may vary, and it is important to ensure that the system performs well under all different conditions. The first case considers load changes from 0.6 A to 1.5 A. The second case considers when the input voltage is 9 V, the load changes from 0.5 to 2 A.

Fig. 18 shows the results for load changes from 0.6 A to 1.5 A and 1.5 A to 0.6 A with the weighting factor ratio $W_r = 2$. As seen, the overshoot and undershoot remain below 1.5 V, with values of approximately 0.5 V, respectively.

Fig. 19 presents the results for an input voltage of 9 V with load changes from 0.5 A to 2 A and a weighting factor ratio of $W_r = 2$. As seen, the overshoot is 1.2 V, which also satisfies the overshoot requirement.

In practice, the load characteristics may not always be purely resistance. To demonstrate the applicability of the proposed method in the studied system with different load characteristics, a validation test involving a constant power load (CPL) is conducted as shown in Fig. 20. The power of the CPL is set to 12 W, and the output voltage undergoes a step change from 12 V to 20 V and leads to a 0.4 A load current variation. To meet the specified overshoot requirement of 1.5 V, a weighting factor $W_r = 1$ is selected.

Upon analysis, it is evident that during dynamic processes caused by the changing output reference, the overshoot (undershoot) is approximately 1.1 V, effectively controlled well within the desired 1.5 V threshold. This successful outcome demonstrates the efficacy of the proposed method in maintaining stable and accurate control of the system under varying load conditions.

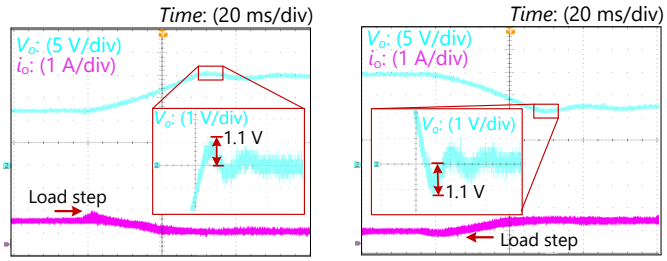

Fig. 20. Output voltage overshoot and undershoot ΔV_o and the output current i_o of the boost converter with $W_r = 1$ and the load power is 12 W. (a) Overshoot of the output voltage when the load current steps down to 0.6 A. (b) Undershoot of the output voltage when the load current steps up to 1 A.

In summary, the results validate that the proposed design method is capable of satisfying the dynamic overshoot requirement under various operating conditions. Specifically, the system exhibits good performance when the load changes, as well as when the input voltage varies to 9 V. In all cases where W_r exceeds 0.7, the overshoot remains consistently below 1.5 V, with values ranging from approximately 1 V to 1.5 V, which are in strict compliance with the design requirement.

V. Conclusion

In conclusion, this paper presents a novel overshoot design method for the MPC controller and validates it with a boost converter system. Based on the proposed method, a minimum weighting factor ratio can be derived for the MPC controller to satisfy the overshoot specification.

The experimental results demonstrate the effectiveness of the proposed design method with a boost converter system by limiting the overshoot during the load current changes with 1.5 A. It proves that as long as the weighting factor ratio W_r is greater than the minimum weighting factor ratio $W_{rm} = 0.7$, the overshoot is less than 1.5 V. Using a larger weighting factor ratio W_r, the overshoot can be further reduced within its adjusting ability. Moreover, the flexible adjustment of the overshoot is realized by simply changing the weighting factor ratio to meet different overshoot design requirements.

Compared to other methods for enhancing the dynamic performance of MPC-controlled systems, the proposed method is intrinsic, does not require any training, and provides flexibility for overshoot regulation, making it applicable to a wide range of MPC-controlled converters.

References

[1] T. Dragičević, X. Lu, J. C. Vasquez, et.al, "DC microgrids—Part I: A review of control strategies and stabilization techniques," *IEEE Trans Power Electron.*, vol. 31, no. 7, pp. 4876-4891, Jul. 2016.

[2] T. Dragičević, S. Vazquez and P. Wheeler, "Advanced Control Methods for Power Converters in DG Systems and Microgrids," vol. 68, no. 7, pp. 5847-5862, July 2021. *IEEE Trans Ind. Electron.*, vol. 68, no. 7, pp. 5847-5862, July 2021.

[3] M. Leng et al., "Small-Signal Stability Assessment and Interaction Analysis for Bipolar DC Microgrids," *IEEE Trans Power Electron.*, vol. 38, no. 4, pp. 5524-5537, April 2023.

[4] B. K. Bose, "Power Electronics, Smart Grid, and Renewable Energy Systems," in *Proc. IEEE*, vol. 105, no. 11, pp. 2011-2018, Nov. 2017.

[5] S. Rivera, S. Kouro, S. Vazquez, S. M. Goetz, R. Lizana and E. Romero-Cadaval, "Electric Vehicle Charging Infrastructure: From Grid to Battery," *IEEE Ind. Electron. Mag.*, vol. 15, no. 2, pp. 37-51, Jun. 2021.

[6] S. Sahoo, T. Dragičević and F. Blaabjerg, "An event-driven resilient control strategy for DC microgrids", *IEEE Trans Power Electron.*, vol. 35, no. 12, pp. 13714-13724, Dec. 2020.

[7] S. Vazquez, J. Rodriguez, M. Rivera, L. G. Franquelo and M. Norambuena, "Model Predictive Control for Power Converters and Drives: Advances and Trends," *IEEE Trans Ind. Electron.*, vol. 64, no. 2, pp. 935-947, Feb. 2017.

[8] S. Vazquez, et al., "Model Predictive Control: A Review of Its Applications in Power Electronics," *IEEE Trans Ind. Mag.*, vol. 8, no. 1, pp. 16-31, March 2014.

[9] Y. Li, S. Sahoo, T. Dragičević, Y. Zhang and F. Blaabjerg, "Stability Oriented Design of Model Predictive Control for DC/DC Boost Converter," *IEEE Trans Ind. Electron.*, vol. 71, no. 1, pp. 922-932, Jan. 2024.

[10] T. Dragičević, "Dynamic Stabilization of DC Microgrids With Predictive Control of Point-of-Load Converters," *IEEE Trans Power Electron.*, vol. 33, no. 12, pp. 10872-10884, Dec. 2018.

[11] L. Chen et al., "Predictive Control Based DC Microgrid Stabilization With the Dual Active Bridge Converter," *IEEE Trans Ind. Electron.*, vol. 67, no. 10, pp. 8944-8956, Oct. 2020.

[12] M. Zhang, Q. Xu, C. Zhang, L. Nordström and F. Blaabjerg, "Decentralized Coordination and Stabilization of Hybrid Energy Storage Systems in DC Microgrids," *IEEE Trans Smart Grid.*, vol. 13, no. 3, pp. 1751-1761, May 2022.

[13] W. Song, M. Zhong, S. Luo and S. Yang, "Model Predictive Power Control for Bidirectional Series-Resonant Isolated DC–DC Converters With Fast Dynamic Response in Locomotive Traction System," *IEEE Trans. Transp. Electrific.*, vol. 6, no. 3, pp. 1326-1337, Sept. 2020.

[14] T. Liu, A. Chen, F. Gao, X. Liu, X. Li and S. Hu, "Double-Loop Control Strategy With Cascaded Model Predictive Control to Improve Frequency Regulation for Islanded Microgrids," *IEEE Trans Smart Grid.*, vol. 13, no. 5, pp. 3954-3967, Sept. 2022.

[15] R. Razani and Y. A. -R. I. Mohamed, "Model Predictive Control of Non-Isolated DC/DC Modular Multilevel Converter Improving the Dynamic Response," *IEEE Open J. Power Electron.*, vol. 3, pp. 303-316, 2022.

[16] D. Zhao et al., "Improved active damping stabilization of DAB converter interfaced aircraft DC microgrids using neural network-based model predictive control", *IEEE Trans. Transp. Electrific*., vol. 8, no. 2, pp. 1541-1552, Jun. 2022.

[17] H. Li, Q. Liu, Z. Zhang, X. Jiang, G. Cao, and Y. Zhang, "A Voltage Overshoot Design Method for DC-DC Converter Based on State Overshoot Concept," *IECON 2021 – 47th Annual Conference of the IEEE Industrial Electronics Society,*, Toronto, ON, Canada, 2021, pp. 1-6.

[18] Texas Instruments, "How to Design a Boost Converter Using the LM5156," 2020. [Online]. Available: https://www.ti.com/lit/ml/snva941a/snva941a.pdf.

[19] USB Implementers Forum, "Battery Charging Specification," 2010. [Online]. Available: https://www.usb.org/document-library/battery-charging-v12-spec-and-adopters-agreement.

[20] European Standards, "BS EN 61851-23:2014 Electric vehicle conductive charging system DC electric vehicle charging station ", 2014. [Online]. Available: https://www.en-standard.eu/bs-en-61851-23-2014-electric-vehicle-conductive-charging-system-dc-electric-vehicle-charging-station/.

[21] European Standards, "DS/EN 16603-20-20 Space engineering – Electrical design and interface requirements for power supply", 2020. [Online] Available: https://www.en-standard.eu/csn-en-16603-20-space-engineering-electrical-and-electronic/.

[22] International organization for standardization, "Road vehicles — Electrical disturbances from conduction and coupling"https://www.iso.org/standard/50925.html," 2011. [Online]. Available: https://www.iso.org/standard/50925.html.

[23] Z. Sun, "Reducing State Overshoot of Switched Linear Systems," *2018 IEEE International Conference on Real-time Computing and Robotics (RCAR)*, Kandima, Maldives, 2018, pp. 321-324.

[24] M. Leng, G. Zhou, Q. Tian, et.al, "Small signal modeling and design analysis for boost converter with valley V2 control," *IEEE Trans Power Electron*., vol. 35, no. 12, pp. 13475-13487, Dec. 2020.

[25] F. C. Lee and Y. Yu, "Input-filter design for switching regulators", *IEEE Trans. Aerosp. Electron. Syst*., vol. AES-15, no. 5, pp. 627-634, Sep. 1979.

[26] Y. Huangfu, S. Pang, B. Nahid-Mobarakeh, L. Guo, A. K. Rathore, and F. Gao, "Stability analysis and active stabilization of on-board DC power converter system with input filter", *IEEE Trans. Ind. Electron*., vol. 65, no. 1, pp. 790-799, Jan. 2018.

[27] L. Cheng, P. Acuna, R. P. Aguilera, et al., "Model predictive control for DC-DC boost converters with reduced-prediction horizon and constant switching frequency," *IEEE Trans Power Electron*., vol. 33, no. 10, pp. 9064-9075, Oct. 2018.

[28] Y. Li, S. Sahoo, Z. Lin, Y. Zhang, T. Dragicevic and F. Blaabjerg, "An Iterative Learning Based Compensation in Model Predictive Control for DC/DC Boost Converter," *25th European Conference on Power Electronics and Applications (EPE'23 ECCE Europe)*, Aalborg, Denmark, 2023, pp. 1-7.

[29] Christophe Basso., "Designing Compensators for the Control of Switching Power Supplies," *Annual IEEE Conference on Applied Power Electronics Conference and Exposition (APEC)*., Seminar, Phoenix, AZ, USA, 2021, pp.1-127.

[30] M. Leng, G. Zhou, Q. Tian, et.al, "Small signal modeling and design analysis for boost converter with valley V2 control," *IEEE Trans Power Electron*., vol. 35, no. 12, pp. 13475-13487, Dec. 2020.

[31] Jian Sun, D. M. Mitchell, M. F. Greuel, P. T. Krein, and R. M. Bass, "Averaged modeling of PWM converters operating in discontinuous conduction mode," *IEEE Trans. Power Electron*., vol. 16, no. 4, pp. 482-492, Jul. 2001.

[32] R. B. Ridley, "A new, continuous-time model for current-mode control (power converters)," *IEEE Trans. Power Electron*., vol. 6, no. 2, pp. 271-280, Apr. 1991.

Yuan Li (Student Member, IEEE) received the B.Sc. & M.Sc. degree in Electrical Engineering from Southwest Jiaotong University, Chengdu, China in 2017 & 2020, respectively. She is currently working toward the Ph.D. degree with AAU Energy, Aalborg University, Aalborg, Denmark. She was a visiting Ph.D. student with the Department of Electronic Engineering, University of Seville, Seville, Spain, in 2023.

Her research interests include modeling of power converters, stability analysis of dc microgrid, and model predictive control for power converters.

Subham Sahoo (Senior Member, IEEE) received the B.Tech. & Ph.D. degree in Electrical and Electronics Engineering from VSSUT, Burla, India and Electrical Engineering at Indian Institute of Technology, Delhi, New Delhi, India in 2014 & 2018, respectively. He is currently an Assistant Professor in the Department of Energy, Aalborg University (AAU), Denmark, where he is also the vice-leader of the research group on Reliability of Power Electronic Converters (ReliaPEC) in AAU Energy. In 2023, he was a visiting professor in the Laboratory of Information and Decision Systems (LIDS), MIT, USA.

He is a recipient of the Indian National Academy of Engineering (INAE) Innovative Students Project Award for the best PhD thesis across all the institutes in India for the year 2019. He is selected into EU-US National Academy of Engineering (NAE) Frontier of Engineering (FOE) Class of 2021. He was also a distinguished reviewer for IEEE Transactions on Smart Grid in 2020. He is currently the vice-chair of IEEE PELS Technical Committee (TC) 10 on Design Methodologies. He is an Associate Editor on IEEE Transactions on Transportation Electrification.

His research interests are control, optimization, cybersecurity and stability of power electronic dominated grids, application of artificial intelligence and machine learning in power systems. systems.

Shuyu Ou (Student Member, IEEE) received the B.S. degree in electrical and automation engineering from South China University, Guangzhou, China, in 2017, the M.Sc. degree in electrical engineering from Royal Institute of Technology, Stockholm, Sweden, in 2019. He worked at Huawei Sweden Research Center, Stockholm, Sweden from 2019 to 2022. Currently, he is a Ph.D. student at Aalborg University, Aalborg, Denmark.

His research interests include reliability study and data-driven condition monitoring of power electronic systems.

Minrui Leng (Student Member, IEEE) received the B.S. degree in electrical engineering and automation from Southwest Jiaotong University, Chengdu, China, in 2014, and the Ph.D. degree from the School of Electrical Engineering, Southwest Jiaotong University, in 2021. From 2019 to 2021, she was a visiting Ph.D. student with the Department of Energy Technology, Aalborg University, Aalborg, Denmark. She is currently an Assistant Professor with the College of Electrical Engineering, Sichuan University, Chengdu, China.

Her research interests include small-signal modeling and dynamical modeling of power converters, control techniques of power converters, stability of distributed power systems and model predictive control, and cyberattacks of dc microgids.

Sergio Vazquez (Fellow, IEEE) was born in Seville, Spain, in 1974. He received the M.S. and Ph.D. degrees in industrial engineering from the University of Seville (US), Seville, Spain, in 2006 and 2010, respectively.

Since 2002, he has been with the Power Electronics Group working on R&D projects. He is an Associate Professor in the Department of Electronic Engineering, US. His research interests include power electronics systems, modeling, modulation, and control of power electronics converters applied to renewable energy technologies.

Dr. Vazquez was recipient as coauthor of the 2012 Best Paper Award of the IEEE Transactions on Industrial Electronics and 2015, 2022 and 2023 Best Paper Award of the IEEE Industrial Electronics Magazine. He is involved in the Energy Storage Technical Committee of the IEEE Industrial Electronics Society and is currently serving as an Associate Editor of the IEEE Transactions on Industrial Electronics.

Tomislav Dragičević (Senior Member, IEEE) received the M.Sc. and the industrial Ph.D. degrees in electrical engineering from the Faculty of Electrical Engineering, University of Zagreb, Zagreb, Croatia, in 2009 and 2013, respectively.

From 2013 until 2016, he has been a Postdoctoral Researcher with Aalborg University, Aalborg, Denmark. From 2016 until 2020, he was an Associate Professor with Aalborg University, Denmark. He is currently a Professor with the Technical University of Denmark, Kongens Lyngby, Denmark. He has authored and coauthored more than 330 technical publications (more than 150 of them are published in international journals, mostly in IEEE), 10 book chapters and a book in this field, as well as filed for several patents. His research interests include application of advanced control, optimization and artificial intelligence inspired techniques to provide innovative and effective solutions to emerging challenges in design, control, and diagnostics of power electronics intensive electrical distribution systems and microgrids.

He serves as an Associate Editor for the IEEE TRANSACTIONS ON INDUSTRIAL ELECTRONICS, IEEE TRANSACTIONS ON POWER ELECTRONICS, IEEE EMERGING AND SELECTED TOPICS IN POWER ELECTRONICS, and IEEE INDUSTRIAL ELECTRONICS MAGAZINE.

Frede Blaabjerg (Fellow, IEEE) was with ABB-Scandia, Randers, Denmark, from 1987 to 1988. From 1988 to 1992, he got the PhD degree in Electrical Engineering at Aalborg University in 1995. He became an Assistant Professor in 1992, an Associate Professor in 1996, and a Full Professor of power electronics and drives in 1998 at AAU Energy. From 2017 he became a Villum Investigator. He is honoris causa at University Politehnica Timisoara (UPT), Romania in 2017 and Tallinn Technical University (TTU), Estonia in 2018.

His current research interests include power electronics and its applications such as in wind turbines, PV systems, reliability, Power-2-X, power quality and adjustable speed drives. He has published more than 600 journal papers in the fields of power electronics and its applications. He is the co-author of eight monographs and editor of fourteen books in power electronics and its applications eg. the series (4 volumes) Control of Power Electronic Converters and Systems published by Academic Press/Elsevier.

He has received 38 IEEE Prize Paper Awards, the IEEE PELS Distinguished Service Award in 2009, the EPE-PEMC Council Award in 2010, the IEEE William E. Newell Power Electronics Award 2014, the Villum Kann Rasmussen Research Award 2014, the Global Energy Prize in 2019 and the 2020 IEEE Edison Medal. He was the Editor-in-Chief of the IEEE TRANSACTIONS ON POWER ELECTRONICS from 2006 to 2012. He has been Distinguished Lecturer for the IEEE Power Electronics Society from 2005 to 2007 and for the IEEE Industry Applications Society from 2010 to 2011 as well as 2017 to 2018. In 2019-2020 he served as a President of IEEE Power Electronics Society. He has been Vice-President of the Danish Academy of Technical Sciences. He is nominated in 2014-2021 by Thomson Reuters to be between the most 250 cited researchers in Engineering in the world.